**Astronomy
&
Astrophysics**

Deep *BVR* imaging of the field of the millisecond pulsar PSR J0030+0451 with the VLT[⋆]

A. B. Koptsevich[1], P. Lundqvist[2], N. I. Serafimovich[1,2], Yu. A. Shibanov[1], and J. Sollerman[2]

[1] Ioffe Physical Technical Institute, Politekhnicheskaya 26, St. Petersburg, 194021, Russia
[2] Stockholm Observatory, AlbaNova, Department of Astronomy, 106 91 Stockholm, Sweden

Abstract. We report on deep *BVR*-imaging of the field of the nearby millisecond pulsar PSR J0030+0451 obtained with the ESO/VLT/FORS2. We do not detect any optical counterpart down to $B \gtrsim 27.3$, $V \gtrsim 27.0$ and $R \gtrsim 27.0$ in the immediate vicinity of the radio pulsar position. The closest detected sources are offset by $\gtrsim 3''$, and they are excluded as counterpart candidates by our astrometry. Using our upper limits in the optical, and including recent *XMM-Newton* X-ray data we show that any nonthermal power-law spectral component of neutron star magnetospheric origin, as suggested by the interpretation of X-ray data, must be suppressed by at least a factor of ~500 in the optical range. This either rules out the nonthermal interpretation or suggests a dramatic spectral break in the 0.003−0.1 keV range of the power-law spectrum. Such a situation has never been observed in the optical/X-ray spectral region of ordinary pulsars, and the origin of such a break is unclear. An alternative interpretation with a purely thermal X-ray spectrum is consistent with our optical upper limits. In this case the X-ray emission is dominated by hot polar caps of the pulsar.

Key words. pulsars: general – pulsars: individual: PSR J0030+0451 – stars: neutron

1. Introduction

Millisecond pulsars (hereafter MSPs) differ from ordinary radio pulsars by much shorter spin periods P, smaller period derivatives $\dot{P}$, higher dynamical ages τ, weaker magnetic fields B, and evolution histories (see, e.g., recent review by Lorimer 2001). Contrary to ordinary pulsars, only 9 of 56 MSPs currently known in the Galactic disk and 25 of 52 MSPs found in globular clusters are isolated objects (Lorimer 2001; Lorimer et al. 2002; Possenti et al. 2001). It is believed that the fast rotation of these neutron stars (NSs) was gained in the past by angular momentum transfer during mass accretion from a companion star (Bhattacharya & van den Heuvel 1991). This was supported by the discoveries of three accretion-powered X-ray MSPs in low-mass X-ray binaries (e.g., SAX J1808.4-3658, see Wijnands & van der Klis 1998).

Despite these differences, the distribution of integrated radio luminosities, as well as the luminosity dependence on P, $\dot{P}$, B, and spindown energy losses $\dot{E}$, are apparently similar for these much older and low-magnetized NSs, and for ordinary pulsars (Kuzmin & Losovsky 2001). About a dozen radio MSPs have been detected in X-rays. It is remarkable that their efficiency in converting spindown energy to X-ray luminosity is roughly the same as for ordinary pulsars, $L_X/\dot{E} \sim 10^{-3}$ (Becker & Trümper 1997; Becker et al. 2000). This suggests that the emission mechanisms responsible for the multi-wavelength radiation of MSPs and ordinary pulsars can be similar, and one could therefore expect to detect MSPs in other spectral ranges as well, as has been done for several ordinary pulsars. Detection of the first MSP in gamma-rays (Kuiper et al. 2000) supports this idea.

To our knowledge, there are still no reports on optical detection of isolated MSPs. It is hardly possible to detect thermal emission from the entire surface of these old, 10^8–10^{10} yr, and cold NSs. However, the spindown energy, expected to power the nonthermal emission of pulsars, can be much higher for MSPs than for old ordinary pulsars, and may even rival that of young pulsars. Assuming the same efficiency of conversion of spindown energy to nonthermal optical luminosity as for ordinary pulsars, one can estimate that nearby MSPs may well be detectable in the optical with large telescopes. A problem is, however, that most of the nearby and energetic MSPs are components of close binary systems where the companion is predominantly either a white dwarf or main sequence star (Lorimer 2001) which outshines the pulsar in the optical. Fortunately, there are at least nine *solitary* MSPs in Galactic disk whose companions are believed to have been either evaporated or ablated (see, e.g., Lommen et al. 2000).

Here we report on deep *BVR* imaging of the field of one of these solitary millisecond pulsars, PSR J0030+0451. This pulsar was only recently discovered with the Arecibo

---

⋆ Based on observations performed at the European Southern Observatory, Paranal, Chile (ESO Programme 67.D-0519).

Table 1. Parameters of PSR J0030+0451 (Lommen et al. 2000; Becker et al. 2000, unless specified otherwise).

		Observed						Derived		
P	$\dot{P}$	$\alpha_{2000}, \delta_{2000}^{a,b}$	μ_α, μ_δ^b	l, b^d	DM^e	τ	B	$\dot{E}$	d^f
ms	10^{-20}		mas yr^{-1}		cm^{-3} pc	Gyr	G	erg s^{-1}	pc
4.865	1.0 ± 0.2	$00^h30^m27\!\!.\!432(9)^c$ $04°51'39\!\!.\!\!''67(2)$	4.1 ± 3.4 -24.6 ± 8.0	$113°\!.1$ $-57°\!.6$	4.3328(2)	7.7	2.2×10^8	3.4×10^{33}	230

^{a} Coordinates are at the epoch of the VLT observations, MJD 52134 (Aug 13, 2001).

^{b} Updated values of the proper motion (A. Lommen 2001, private communications).

^{c} Numbers in parentheses are uncertainties referring to the last significant digit quoted.

^{d} Galactic coordinates.

^{e} Dispersion measure.

^{f} *DM*-based distance (the new distance model by Cordes & Lazio 2002 places the pulsar to 317 pc).

telescope (Lommen et al. 2000), and soon thereafter detected in X-rays during the final observations with the *ROSAT/PSPC* (Becker et al. 2000). Recently it was re-observed in X-rays with the *XMM-Newton* (Becker & Aschenbach 2002). This relatively nearby NS (see Table 1 for its parameters) is characterized by high X-ray flux, about $(4.3-6.8) \times 10^{-13}$ erg s^{-1} cm^{-2} in the 0.1–2.4 keV band, and low interstellar absorption, $N_H \lesssim 3 \times 10^{20}$ cm^{-2}, corresponding to a color excess $E(B-V) \lesssim 0.06$ mag. This makes it a promising candidate for optical detection. In Sect. 2 we present the observations and the data reduction. In Sect. 3 we discuss our results in the optical in conjunction with the available X-ray data.

2. Observations and data reduction

The field of PSR J0030+0451 was observed in service mode on July 26 and August 13, 2001, with the FOcal Reducer/low dispersion Spectrograph (FORS2) on the ESO/VLT/UT2 telescope[1], with a pixel scale of $0\!\!.\!\!''2$. We used Bessel filters for *B* and *V*, and an ESO special filter for *R* ($R_{special}$, henceforth called R_s)[2]. Unfortunately, some of the *V* images were corrupted by bad CCD columns near the expected position of the pulsar and were not used in the analysis. The images we used are listed in Table 2.

Bias subtraction and flatfielding were performed in a standard way, and the reduced individual images were aligned using a set of bright, non-saturated field stars. Standard utilities from the NOAO IRAF package were then used to combine the images applying the averaged sigma clipping algorithm avsigclip with the scale parameter equal to none. The pulsar vicinity is shown for *B*, *V* and R_s bands in Fig. 1.

The radio position of PSR J0030+0451 at the epoch of the VLT observations (for which 13.08.01 was adopted, see Table 1) was determined using recent radio ephemerides (A. Lommen 2001, private communication for additional Arecibo observations). Astrometrical referencing of our images was made with IRAF tasks ccmap/cctran using the positions of several dozens of reference stars from the USNO A-2.0

Table 2. Log of VLT observations of PSR J0030+0451 in the BVR_s bands. Exposure time is 720 s for all frames.

No.	Date UT	Band	Time UT	Airmass	Seeing arcsec
1	26.07.01	*B*	09:40	1.172	0.6
2			09:53	1.188	0.5
3	13.08.01	*B*	04:55	1.579	1.1
4			05:09	1.495	1.1
5			06:34	1.208	0.8
6			07:56	1.150	0.7
7			08:09	1.155	0.9
8		*V*	05:38	1.358	0.7
9			05:52	1.311	0.8
10			06:06	1.269	0.8
11			07:14	1.159	0.7
12			07:28	1.151	0.6
13			07:42	1.149	0.7
14		R_s	06:47	1.187	0.7
15			08:24	1.167	0.7
16			08:37	1.181	0.7
17			08:53	1.205	0.7
18			09:07	1.230	0.7

catalogue seen in the images and optimizing the astrometrical fit by removing step by step the reference stars with the largest residuals. For the 5 most suitable stars we finally got 1σ rms-errors of $0\!\!.\!\!''05$ and $0\!\!.\!\!''11$, and maximum residuals of $0\!\!.\!\!''20$ and $0\!\!.\!\!''24$, in RA and Dec, respectively. Combining the rms-errors with the nominal USNO accuracy of $0\!\!.\!\!''24$ and radio ephemeris uncertainties, we obtained the 3σ pulsar VLT/FORS position uncertainties $0\!\!.\!\!''79$ and $0\!\!.\!\!''88$ in RA and Dec, respectively. The resulting 3σ error ellipse is marked in the smaller images in Fig. 1. No reliable counterpart candidate was detected within, or close to the error ellipse of the expected pulsar position. We also double-checked the astrometry with 5 stars from the GSC-II catalog. The obtained rms errors were $0\!\!.\!\!''05$ and $0\!\!.\!\!''11$ in RA and Dec, respectively, and the expected pulsar position was moved $0\!\!.\!\!''06$ west and $0\!\!.\!\!''14$ north in respect to the USNO position. However, since the main source of errors is the catalog uncertainty, we accept the USNO results as more conservative estimate.
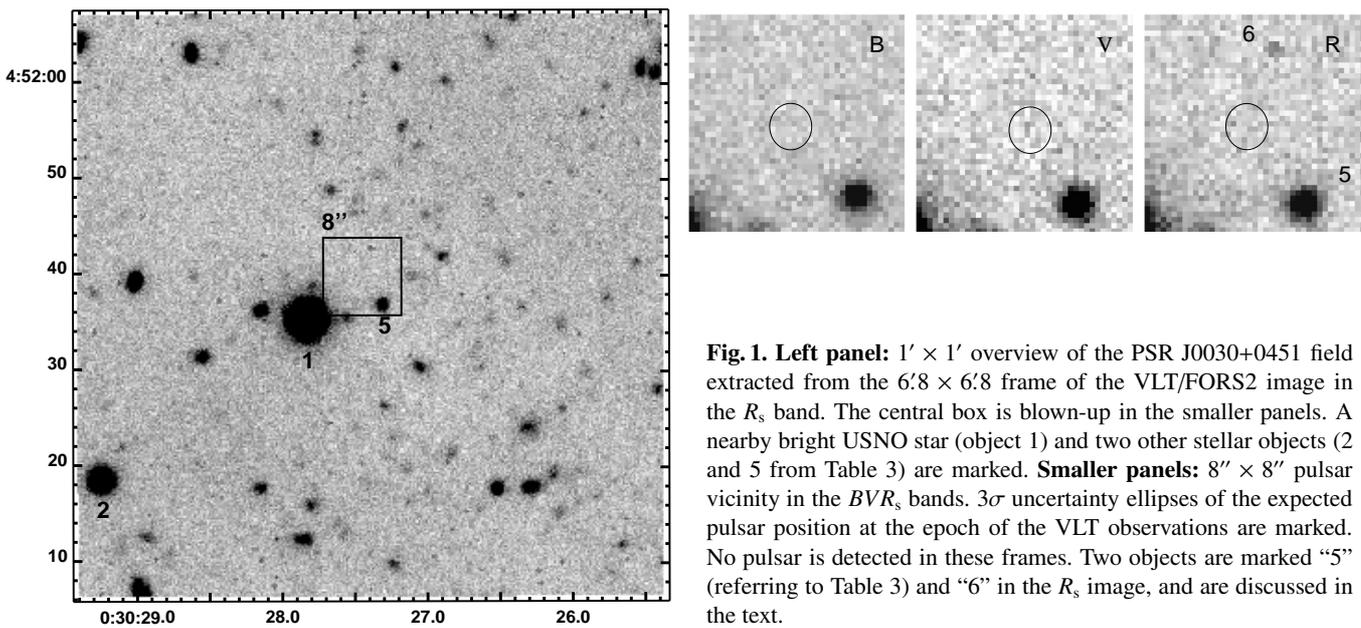
---

[1] See http://www.eso.org/instruments/fors/ for details on the instrument.

[2] See http://www.eso.org/instruments/fors1/Filters/

Fig. 1. Left panel: $1' \times 1'$ overview of the PSR J0030+0451 field extracted from the $6\rlap{.}'8 \times 6\rlap{.}'8$ frame of the VLT/FORS2 image in the $R_{\rm s}$ band. The central box is blown-up in the smaller panels. A nearby bright USNO star (object 1) and two other stellar objects (2 and 5 from Table 3) are marked. **Smaller panels:** $8'' \times 8''$ pulsar vicinity in the $BVR_{\rm s}$ bands. 3σ uncertainty ellipses of the expected pulsar position at the epoch of the VLT observations are marked. No pulsar is detected in these frames. Two objects are marked "5" (referring to Table 3) and "6" in the $R_{\rm s}$ image, and are discussed in the text.

Table 3. Magnitudes of several stars in the PSR J0030+0451 field with coordinates and offsets from the pulsar position shown in the table. Stars 1, 2 and 5 are marked within the left frame in Fig. 1, while 3 and 4 are outside this frame.

No.	α_{2000}	δ_{2000}	Offset	B	V	$R_{\rm s}$
1	00:30:27.83	+04:51:35.2	$7\rlap{.}''5$	19.20±0.01	–	–
2	00:30:29.25	+04:51:18.3	$34\rlap{.}''6$	22.32±0.02	20.92±0.01	20.27±0.01
3	00:30:39.33	+04:53:15.4	$3'21\rlap{.}''9$	23.77±0.06	22.08±0.01	21.29±0.01
4	00:30:25.39	+04:53:14.2	$1'39\rlap{.}''3$	24.15±0.07	22.40±0.02	21.78±0.01
5	00:30:27.32	+04:51:36.9	$3\rlap{.}''2$	23.82±0.05	23.69±0.06	23.63±0.06
PSR	00:30:27.43	+04:51:39.67	–	≥27.3	≥27.0	≥27.0

For the photometric calibrations we used the photometric standards from the PG1323−085 and SA109 fields (Landolt 1992), observed at the second night of our observations, and average Paranal extinction coefficients[3]. We then derived 3σ detection limits as $m = -2.5 \log\left(3\sigma \sqrt{A}/T_{\rm exp}\right) + m_0$, where σ is the standard deviation of the flux in counts per pixel, $T_{\rm exp}$ is the exposure time, A is the area of an aperture (in pix^2) with a radius of $1''$ (corresponding to ~83% of the flux in a PSF of our images), and m_0 is the photometric zeropoint, including corrections for atmospheric extinction. The limits are: $B = 27.3$, $V = 27.0$, and $R_{\rm s} = 27.0$.

In Table 3 we list $BVR_{\rm s}$ magnitudes for several of the objects in the PSR J0030+0451 field. Object 1 is the USNO star U0900_00118426 marked in the left panel of Fig. 1. It is oversaturated in our V and $R_{\rm s}$ images. Object 5 is the source seen at the bottom right of the blown-up images in Fig. 1. This is the closest object to the radio position of the pulsar clearly detected in all our images. Although it is too blue to be a normal star, it cannot be considered a pulsar counterpart candidate because of the large offset ($3\rlap{.}''4$) from the radio position, provided the radio astrometry is as accurate as claimed by Lommen et al. (2000). Like most other blue objects in the field at this magnitude level (we found at least five objects roughly of the same

color), it is most likely extragalactic, and similar to blue objects found in the HDF images. The object marked "6" in the upper right of the $R_{\rm s}$ image in Fig. 1, is only marginally detected at $R_{\rm s} = 27.45 \pm 0.61$. It is not detected in the other bands and may well be an artefact of the reductions. It is also too far ($3\rlap{.}''1$) from the radio pulsar position to be an optical counterpart candidate.

3. Discussion

Based on the apparent similarity of the radiation properties of MSPs and ordinary pulsars, and assuming the same mechanisms to generate optical emission in both types of pulsar, we expected to detect the optical counterpart of PSR J0030+0451 at the $m \sim 26$ visual magnitude level, assuming a simple scaling of $\dot{E}/d^2$ from known optical fluxes of ordinary pulsars. Our observations were deeper, but still we did not detect any reliable counterpart candidate.

To try to understand what our optical non-detection implies, we have plotted the available information about the multiwavelength spectrum of PSR J0030+0451 including radio, optical, and X-ray data in Fig. 2. For the X-ray region we have included preliminary results of recent *XMM-Newton* observations (Becker & Aschenbach 2002) where the pulsar was clearly detected in the 0.3−7 keV range. The detection range is shown by a horizontal bar with arrows in Fig. 2. The overall spectrum compares well with multiwavelength spectra of

---

[3] http://www.eso.org/observing/dfo/quality/FORS2/qc/photcoeff/photcoeffs_fors2.html

ordinary pulsars (e.g., Koptsevich et al. 2001), i.e., the pulsar flux is higher in the radio and fades toward the X-ray range. This can be explained by different emission mechanisms in the radio (coherent) and at shorter wavelengths (non-coherent). However, a more detailed inspection of the optical/X-ray range reveals a feature which has not been seen for ordinary pulsars. For the latter, the optical flux is usually close to an extrapolation of the nonthermal high energy tail of the X-ray emission, usually described by a power-law (PL). From Fig. 2 it is clear that this is not the case for the PSR J0030+0451.

Figure 2 shows that in the *XMM-Newton* range the data can be fitted equally well by three different two-component spectral models: a blackbody + power-law model (BB+PL), a broken (or curved) PL model, or a model based on two different blackbodies (BB+BB) with $N_{\rm H} \leq 2.5 \times 10^{20}$ cm^{-2}. From the X-ray data alone it is difficult to discriminate between the three models, although the sharp X-ray pulse profile perhaps favors the domination of a nonthermal PL component (Becker & Aschenbach 2002). The VLT upper limits allow additional constraints using an extrapolation of the X-ray model spectra toward the optical range.

From Fig. 2 it is seen that the low-energy extension of the BB+PL fit overshoots the optical flux upper limits of PSR J0030+0451 by ~5 orders of magnitude. The broken PL extension, which implies a flatter spectrum in the soft X-ray energy band, is also 3-4 orders of magnitude higher. We have not corrected the data for interstellar extinction, which is low and does not play any significant role at such large differences. The strong suppression of the PL components in the optical range suggests that these two models either should be ruled out, or that their PL components must have a strong break or even a cutoff at a photon energy somewhere in the $0.003-0.1$ keV range. Such a situation has never been observed for any ordinary pulsar. For example, the spectral index α_ν (defined as $F_\nu \propto \nu^{-\alpha_\nu}$) of the young Crab pulsar changes from ~0.5 for soft X-rays to zero in the FUV/optical/near-IR range (e.g., Sollerman et al. 2000; Sollerman & Flyckt 2002). For the relatively young Vela-pulsar (Mignani & Caraveo 2001), the middle-aged PSR B0656+14 (Koptsevich et al. 2001) and PSR B1055−52 (Pavlov et al. 2002), and even for the old ordinary pulsars PSR B0950+08 (Zharikov et al. 2002) and PSR B1929+10 (Mignani et al. 2002a), the extension of the PL X-ray component matches the optical flux, suggesting the same mechanism of nonthermal emission in the optical and X-ray ranges. It is not clear what could be the reason for such a strong change in the nonthermal spectral slope of PSR J0030+0451 from negative in X-rays to positive in the optical range. As seen from Fig. 2, the X-ray PL fits and our upper limits exclude any flat extension toward the optical range, even if we place a break point energy at the lower boundary of the *XMM-Newton* range ~0.1 keV. Note that the low-frequency extensions of the PL components overshoot even the radio fluxes. This is also not typical for ordinary pulsars. One can assume that nonthermal emission is due to synchrotron radiation of relativistic particles in the magnetosphere of the pulsar. In this case we obtain for the simplest monochromatic particle distribution over the energy a spectral flux of $F_\nu \propto \nu^{1/3}$ in the low frequency range below a maximum frequency $\nu_{\rm m} \propto B\gamma^2$. Here B is the

magnetic field, and γ is the gamma-factor of the emitting particles. From the spectral shape suggested by the X-ray data and optical upper limits it is natural to put $\nu_{\rm m}$ near the maximum of the X-ray spectral flux at the low boundary of the *XMM-Newton* range. At typical gamma-factors of primary and secondary relativistic particles in pulsar magnetospheres, i.e. ~10^6 and ~10, respectively, and for the period of PSR J0030+0451 ~4.9 ms, the same peak frequency value is predicted by a model of synchrotron emission from the pulsar light cylinder suggested by Malov (2001). For the expected synchrotron flux below the adopted $\nu_{\rm m}$ value (see Fig. 2, dotted lines) we would likely hint the optical counterpart, but we did not.

The purely thermal BB+BB spectral model is consistent with our upper limits without any additional assumptions. Its Rayleigh-Jeans tail is about 6 stellar magnitudes fainter in the optical than our upper limits, and would hardly be detectable with present telescopes. Thermal photons can be emitted by hot polar caps of the pulsar. The two-blackbody fit indicates a non-uniformity in the temperature distribution over the caps. This could be described by heat propagation over the surface of the neutron star out of a hot cap core, including neutron star atmosphere effects, as has been done in the case of the MSP J0437−4715 (Zavlin et al. 2002). An additional faint PL component is required to fit an excess over the thermal emission at high energy X-rays from PSR J0437−4715. If the same would be true for PSR J0030+0451, it could be brighter in the optical than estimated from the simple BB+BB model due to a contribution from a similar nonthermal component of magnetospheric origin. Deeper X-ray observations are probably needed to detect this component in the high energy tail of the PSR J0030+0451 spectrum. The similarity of X-ray and radio pulse profiles of this pulsar suggests that radio and X-ray peaks are in phase (Becker & Aschenbach 2002), although direct timing to confirm this has not yet been done. In the frame work of the thermal model this means that radio emission is generated close to the polar cap surface and the similarity of the pulse shapes is likely caused by the same geometry of the emitting regions.

Based on our upper limits we can constrain also the efficiency of converting spindown power of PSR J0030+0451 to optical emission. The luminosity in the B band is $L_B = 4\pi d^2 F_B \Delta \nu_B \lesssim 6.3 \times 10^{26} d_{230}^2$ erg s^{-1}, and hence the optical efficiency $\eta_B = L_B/\dot{E} \lesssim 1.9 \times 10^{-7} d_{230}^2$. Here $d_{230} = d/230$ pc is the normalized distance to PSR J0030+0451. This upper limit is about half the efficiency of the middle-aged PSR B0656+14 (at 500 pc) and exceeds the efficiencies of the Geminga and Vela pulsars by about 1 and 2 orders of magnitude, respectively (see, e.g., Zharikov et al. 2002). It is interesting to note that the expected efficiency in the BB+BB model in Fig. 2 is 2–3 orders of magnitude lower than the upper limit derived above from our optical data, and that the efficiency in the BB+BB model is comparable to that of the Vela pulsar. The comparison of the efficiencies makes sense here, since the thermal emission from hot polar caps and the nonthermal magnetospheric emission of the Vela-pulsar, both are powered by relativistic particles produced in magnetospheres of rapidly rotating NSs. Thus, we see that the optical efficiency of the PSR J0030+0451, as derived from our and X-ray observations, is not unusually low, but is
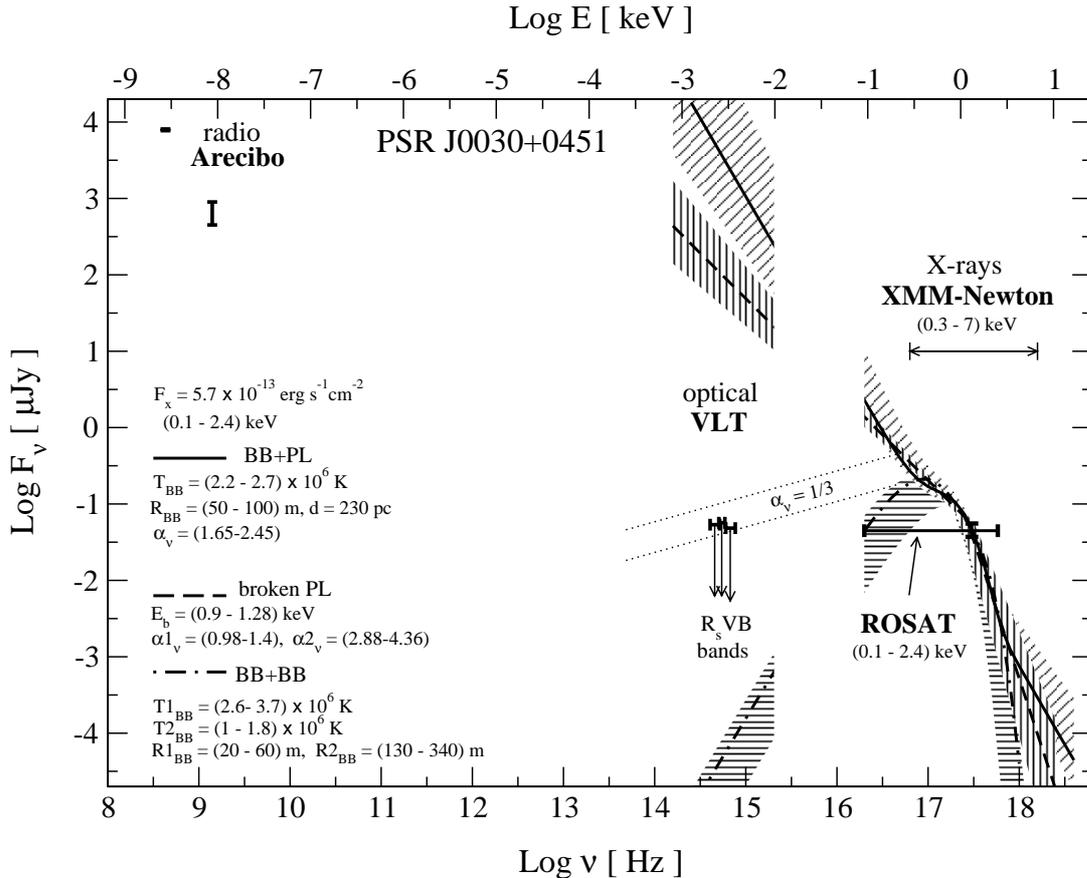
Fig. 2. Radio and X-ray observations of PSR J0030+0451 with the Arecibo telescope (Lommen et al. 2000), *ROSAT* (Becker et al. 2000), and *XMM-Newton* (Becker & Aschenbach 2002), as well as VLT upper limits in the *BVR*$_{\rm s}$ optical bands. Solid, dashed, and dot-dashed lines show the best spectral fits of the *XMM-Newton* data with three alternative two component spectral models: BB+PL, broken PL, and BB+BB, respectively (BB stands for blackbody). Parameters of the fits and a mean unabsorbed integrated flux $F_{\rm X}$, approximately the same for all the fits (Becker & Aschenbach 2002), are indicated in the plot. All fits are acceptable at the same significance level in the $\sim 0.3 - 7$ keV range, indicated by a horizontal bar with arrows at the upper-left, and their $\sim$90% uncertainties are shown as shaded regions. The unabsorbed model spectra are extrapolated toward the optical range. Previous *ROSAT* data contain no spectral information and provide only an integrated flux indicated in the figure by a bold cross (Becker et al. 2000), roughly consistent with the more recent *XMM-Newton* results. The VLT upper limits, marked by end bars, show that any nonthermal PL component obtained from the above spectral fits of the X-ray data must be strongly suppressed in the optical range. This implies either a cutoff or a strong break in the 0.003−0.1 keV range. The purely thermal BB+BB model is consistent with our optical upper limits. Further details of this plot are discussed in Sect. 3.

compatible with the efficiency range of ordinary pulsars detected in the optical band.

It has been shown for ordinary pulsars that spectral index appears to became steeper with pulsar age in the optical range (Koptsevich et al. 2001; Mignani & Caraveo 2001), while it flattens in gamma rays (e.g., Shearer & Golden 2002). It has been noticed also across a restricted set of young and middle-aged pulsars detected in the optical and gamma regions that the gamma-ray efficiency increases with age, while the reverse is true for the optical efficiency (Goldoni et al. 1995). This would suggest that there is a reprocessing of the gamma-photons into the optical in pulsar magnetospheres, and that it is more efficient for younger pulsars than for older ones (e.g., Shearer & Golden 2002). Thus, it would be not surprising that very old PSR J0030+0451 is fainter in the optical than we expected. However, recent optical studies of old ordinary pulsars (Zharikov et al. 2002; Mignani et al. 2002a,b) have revealed nonmonotonous behavior of the optical efficiency vs.

age with a minimum at $\tau \sim 10^4$–10^5 yr and further increase towards higher ages $\tau \gtrsim 10^7$ yr. Old pulsars can be actually much more efficient than the middle-aged ones and produce the optical photons with almost the same efficiency as young and energetic Crab-like pulsars. In this context low optical brightness of the MSP J0030+0451 remains puzzling.

A clue to what dominates the X-ray and optical spectrum would hopefully be found from observations of PSR J0030+0451 and other MSPs in the FUV and, in particular, in the EUV range. Even deep upper limits in these ranges would help to understand how strongly the multiwavelength emission and radiation properties of MSPs differ from those of ordinary pulsars.

References

Becker, W., & Trümper, J. 1997, A&A, 326, 682

Becker, W., & Trümper, J. 1999, A&A, 341, 803

Becker, W., Trümper, J., Lommen, A. N., & Backer, D. C. 2000, ApJ, 545, 1015

Becker, W., & Aschenbach, B. 2002, in the Proceedings of the 270. WE-Heraeus Seminar on Neutron Stars, Pulsars and Supernova Remnants. MPE Report 278, ed. W. Becker, H. Lesch & J. Trümper, 64 [astro-ph/028466]

Bhattacharya, D., & van den Heuvel, E. P. J. 1991, Phys. Rep., 203, 1

Cordes, J. M., & Lazio, T. J. W. 2002 [astro-ph/0207156]

Goldoni, P., Musso, C., Caraveo, P. A., et al. 1995, A&A, 298, 535

Koptsevich, A. B., Pavlov, G. G., Zharikov, S. V., et al. 2001, A&A, 370, 1004

Kuiper, L., Hermsen, W., Verbunt, F., et al. 2000, A&A, 359, 615

Kuzmin, A. D., & Losovsky, B. Ya. 2001, A&A, 368, 230

Landolt, A. 1992, AJ, 104, 340

Lommen, A. N., Zepka, A., Backer, D. C., et al. 2000, ApJ, 545, 1007

Lorimer, D. R. 2001, Article in Online Journal Living Reviews in Relativity, vol. 4, http://www.livingreviews.org/Articles/Volume4/2001-5lorimer/index.html)

Lorimer, D. R., Camilo, F., Freire, P., et al. 2002, in Proc. Conf. Radio Pulsars, Chania, Crete, Sep. 2002 [astro-ph/0210460]

Malov, I. F. 2001, Astron. Rep., 45, 863

Mignani, R. P., & Caraveo, P. A. 2001, A&A, 376, 213

Mignani, R. P., De Luca, A., Caraveo, P. A., & Becker, W. 2002a, ApJ, 580, L147

Mignani, R., Manchester, R., & Pavlov, G. G. 2002b, ApJ, submitted [astro-ph/0209268]

Pavlov, G. G., Zavlin, V. E., & Sanwal, D. 2002, in the Proceedings of the 270. WE-Heraeus Seminar on Neutron Stars, Pulsars and Supernova Remnants. MPE Report 278, ed. W. Becker, H. Lesch, & J. Trümper, 273 [astro-ph/0206024]

Possenti, A., D'Amico, N., Manchester R. N., et al. 2001 [astro-ph/0108343]

Shearer, A., & Golden, A. 2002, in the Proceedings of the 270. WE-Heraeus Seminar on Neutron Stars, Pulsars, and Supernova Remnants. MPE Report 278, ed. by W. Becker, H. Lesch, & J. Trümper, 44 [astro-ph/0208579]

Sollerman, J., Lundqvist, P., Lindler, D., et al. 2000, ApJ, 537, 861

Sollerman, J., & Flyckt, V. 2002, Messenger, 107, 32

Wijnands, R., & van der Klis, M. 1998, Nature, 394, 344

Zavlin, V. E., Pavlov, G. G., Sanwal, D., et al. 2002, ApJ, 569, 894

Zharikov, S. V., Shibanov, Yu. A., Koptsevich, A. B., et al. 2002, A&A, 394, 633